Mon. Not. R. Astron. Soc. **000**, 1–10 (2008) Printed 26 March 2014 (MN LATEX style file v2.2)

Intermediate mass black holes in AGN disks II. Model predictions and observational constraints

B. McKernan[1,2,3,4⋆], K.E.S. Ford[1,2,3,4], B.Kocsis[5,6],W.Lyra[7,8,10], L.M.Winter[9]
[1]*Department of Science, Borough of Manhattan Community College, City University of New York, New York, NY 10007, USA*
[2]*Department of Astrophysics, American Museum of Natural History, New York, NY 10024, USA*
[3]*Graduate Center, City University of New York, 365 5th Avenue, New York, NY 10016, USA*
[4]*Kavli Institute for Theoretical Physics, UC Santa Barbara, CA 93106, USA*
[5]*Harvard-Smithsonian Center for Astrophysics, 60 Garden St., Cambridge, MA 02138, USA*
[6]*Institute for Advanced Study, Einstein Drive, Princeton, NJ 08540*
[7]*Jet Propulsion Laboratory, California Institute of Technology, 4800 Oak Grove Dr., Pasadena, CA 91109, USA*
[8]*California Institute of Technology, Division of Geological & Planetary Sciences, 1200 E. California Blvd., Pasadena, CA 91125, USA*
[9]*Center for Astrophysics & Space Astronomy, University of Colorado, Boulder, CO 80303, USA*
[10]*Sagan Fellow*

arXiv:1403.6433v1 [astro-ph.GA] 25 Mar 2014

Accepted. Received; in original form

ABSTRACT
If intermediate mass black holes (IMBHs) grow efficiently in gas disks around supermassive black holes, their host active galactic nucleus (AGN) disks should exhibit myriad observational signatures. Gap-opening IMBHs in AGN disks can exhibit spectral features and variability analagous to gapped protoplanetary disks. A gap-opening IMBH in the innermost disk imprints ripples and oscillations on the broad Fe Kα line which may be detectable with future X-ray missions. A non-gap-opening IMBH will accrete and produce a soft X-ray excess relative to continuum emission. An IMBH on a retrograde orbit in an AGN disk will not open a gap and will generate soft X-rays from a bow-shock 'headwind'. Accreting IMBH in a large cavity can generate ULX-like X-ray luminosities and LINER-like optical line ratios from local ionized gas. We propose that many LINERs house a weakly accreting MBH binary in a large central disk cavity and will be luminous sources of gravitational waves (GW). IMBHs in galactic nuclei may also be detected via intermittent observational signatures including: UV/X-ray flares due to tidal disruption events, asymmetric X-ray intensity distributions as revealed by AGN transits, quasi-periodic oscillations and underluminous Type Ia supernovae. GW emitted during IMBH inspiral and collisions may be detected with eLISA and LIGO, particularly from LINERs. We summarize observational signatures and compare to current data where possible or suggest future observations.

Key words: galaxies: active – (stars:) binaries:close – planets-disc interactions – protoplanetary discs – emission: accretion

1 INTRODUCTION

There is overwhelming observational evidence for supermassive black holes (SMBH;$> 10^6 M_\odot$) in the centers of galaxies (Kormendy & Richstone 1995) and stellar mass black holes ($< 20 M_\odot$) in our own Galaxy (Remillard & McClintock 2006). However, there is only fragmentary evidence for intermediate mass black holes (IMBHs, see Davis et al. 2011 for the best candidate to date). IMBHs are thus a key missing component of our Universe. The standard model of IMBH production is in clusters (Miller & Hamilton 2002), however there are currently no undisputed cases of IMBHs in globular clusters (Strader et al. 2012); IMBHs are hard to find.

In McKernan et al. (2012) (Paper I), we described a model for the production and growth of IMBH seeds in disks around supermassive black holes. Our model grows IMBH seeds at super-Eddington rates in disks in active galactic nuclei (AGN). IMBH growth occurs both via collision of stars and compact objects at low relative velocity in disks (core accretion) and via gas accretion as the IMBH migrates within the disk. Our model is analagous to the growth of giant planets in protoplanetary disks (e.g. Pollack et al. 1996; Armitage 2010) and grows IMBHs more efficiently than the standard model (Miller & Hamilton 2002). In this paper we out-

⋆ E-mail:bmckernan at amnh.org (BMcK)

© 2008 RAS

line the wide range of predicted observables that can reveal IMBHs in galactic nuclei throughout the local Universe.

In Section §2 we discuss conditions in the AGN disk under which IMBHs can open a gap. In Section §3 we discuss observational consequences of gaps in the outer AGN disk. We draw a parallel between observational signatures of gapped protoplanetary disks and gaps carved out by IMBHs in AGN disks. In section §4 we outline the effect of a gap-opening IMBH in the inner AGN disk on the broad component of the FeKα line, which yields signatures that allow us to follow the final stage of mergers and provides advance warning of gravitational wave outbursts. In Section §5 we discuss the signatures of accreting IMBHs in AGN disks. In Section §6 we discuss occasional signatures of IMBHs in galactic nuclei. In section §7 we discuss gravitational wave signatures of our model potentially detectable with LIGO and LISA.

2 GAP-OPENING IN AGN DISKS

Gap opening in any accretion disk depends on the ratio of satellite mass (M_2) to primary mass (M_1) , disk viscosity and the disk aspect ratio. A simple estimate of the critical mass ratio ($q = M_2/M_1$), above which the IMBH will open a gap in the disk, is given by (Lin & Papaloizou 1986)

$$q \approx \left(\frac{27\pi}{8}\right)^{1/2} \left(\frac{H}{r}\right)^{5/2} \alpha^{1/2} \quad (1)$$

where (H/r) is the disk thickness and α is the viscosity parameter (Shakura & Sunyaev 1973). The pre-factor can differ by up to an order of magnitude depending on the approximations used in calculating the torque (Crida et al. 2006), however for most disk models eqn. (1) is sufficient to estimate the minimum gap-opening mass (Edgar et al. 2007). Clearly, only IMBH or larger mass BH can open gaps in AGN disks. In particular, to open a gap requires low disk viscosity such that (Crida et al. 2006)

$$\alpha < 0.09 q^2 \left(\frac{H}{r}\right)^{-5}. \quad (2)$$

Even if an IMBH is sufficiently massive to open a gap in a disk ($q > 10^{-4}$ typically), the gap can close by pressure if the disk is geometrically thick enough such that (Bryden et al. 1999)

$$\frac{H}{r} > \frac{1}{40} \left(\frac{q}{\alpha}\right)^{1/2}. \quad (3)$$

Combining these conditions allows gap opening to occur when $H/r \lesssim \min[(1/40)(q/\alpha)^{1/2}, (q^2/\alpha)^{1/5}]$. Thus, any gap detection can tell us a lot about AGN disks. We do not address in detail the recent result from (Zhu et al. 2013) that low-mass satellites may open gaps in a disk but note that in hot AGN disks, where MRI is effective, even IMBH with $q < 10^{-4}$ may open gaps.

Just before gap-opening occurs, the disk perturbation may allow for very rapid Type III migration (Masset & Papaloizou. 2003; Pepliński et al. 2008a,b) with consequences for observed AGN luminosity (McKernan et al. 2011a). Once a gap opens, the outer edge of the gap is exposed to the central radiation source and both the inner edge and the disk immediately outside the outer edge are shadowed, leading to a change in the observed spectral energy distribution (e.g. Jang-Condell & Sasselov 2003; Espaillat et al. 2007) (and see §3 below). The gap will be approximately $2R_H$ in width where $R_H = a(q/3)^{1/3}$ is the IMBH Hill radius and a the IMBH semi-major axis. The gap is not completely empty as the IMBH is fed by leading and trailing resonance arms (analagous to gap-opening Jupiters in protoplanetary disks) and the IMBH may have an accretion disk of size-scale $R \ll R_H$ (Hayasaki et al. 2008; Roedig et al. 2012; D'Orazio et al. 2013). A gap-opening IMBH migrates within the disk on the so-called Type II migration timescale given by

$$\tau_{\rm II} = \frac{1}{\alpha} \left(\frac{H}{r}\right)^{-2} \frac{1}{\omega} \quad (4)$$

where ω is the Keplerian angular frequency and $\tau_{\rm II} = \tau_\alpha$, the viscous disk timescale.

The coevolution of an AGN disk with an IMBH can differ from that of planets in a protoplanetary disk. First, the Type II migration rate varies depending on the ratio of the gas to radiation pressure in the inner AGN disk, since this influences (H/r) and α. Second, the mass of the IMBH may be larger than the local disk mass in the radiation pressure dominated regime. In this case, the disk banks up on the outer edge of the gap before it can push the IMBH inwards (Syer & Clarke 1995; Ivanov et al. 1999; Kocsis et al. 2012a). The viscous timescale is smallest inside the orbit of the IMBH, so the inner disk can drain away, leaving an empty central cavity (Artymowicz & Lubow 1996; Kocsis et al. 2012b). The viscous disk will pile-up just outside the IMBH orbit, analagous to the build-up of water behind a dam. The dam may leak or burst after a time, refilling the inner disk and leaving an annulus in the disk and/or an accreting IMBH (e.g. Kocsis et al. 2012a; McKernan et al. 2013; D'Orazio et al. 2013; Farris et al. 2013, & references therein). Third, GW emission by the IMBH eventually dominates over Type II migration. If there is a circular cavity in the disk, once the GW timescale becomes shorter than the viscous time, the outer edge of the gap cannot follow the IMBH and effectively freezes until the binary merges (Armitage & Natarajan 2002; Liu et al. 2003; Milosavljevic & Phinney 2005). However, if there is an inner disk as the IMBH inspirals due to GW emission, the gap may retain an annular geometry with characteristic width $\sim R_{\rm H}$ tracking the inspiralling IMBH (Baruteau et al. 2012, see however Chang et al. 2010). Only IMBH or SMBH can open gaps in AGN disks, so the detection of gaps in disks will set excellent constraints on $(H/r), \alpha$ in models of AGN disks (Ivanov et al. 1999; Hayasaki et al. 2008; Rafikov 2012; Kocsis et al. 2012a), in spite of uncertainties in those models.

3 GAPS & CAVITIES IN OUTER AGN DISKS: PREDICTIONS

Our model of IMBH growth displays strong parallels with models of giant planet growth in protoplanetary disks. A large fraction ($> 1/5$) of protoplanetary disks exhibit evidence for gaps or cavities probably carved out by giant protoplanets (e.g. Andrews et al. 2011, and references therein). If AGN disk conditions permit an IMBH to carve out a gap or cavity, the AGN should display features and variability analagous to those in gapped protoplanetary disks.

3.1 SED dip: predictions

Consider an AGN disk consisting of annuli, each at a different temperature. In an AGN disk without a gap, each of the annuli contributes a black body spectrum to the overall multi-colour optical/UV spectrum. If the AGN disk includes a gap, then the black body spectrum due to that missing annulus is subtracted from the overall spectrum, leading to a dip or break around that disk temperature (Gültekin & Miller 2012), independent of breaks due to

reddening or absorption edges (e.g. Zheng et al. 1995) . From protoplanetary disk theory, the width of the gap (w) will be $w \geqslant 2R_H = 2(q/3)^{1/3}a \sim 0.07(0.14)a$, for $q = 10^{-4}(10^{-3})$ (Armitage 2010), where a is the semi-major axis of the IMBH orbit.

The spectral break wavelength (λ_b) due to a fully empty blackbody annulus in a homogeneous thin disk around a SMBH of mass M accreting at rate $\dot{M}$ is

$$\lambda_b = \left(\frac{hc}{xk}\right)\left(\frac{G}{2\pi\sigma}\right)^{-1/4}\left(\frac{M\dot{M}}{r^3}\right)^{-1/4} \quad (5)$$

where $x \sim 5$ and we rewrite λ_b as

$$\lambda_b \sim 140\eta^{1/4}\left(\frac{r_2}{r_g}\right)^{3/4}\left(\frac{M_1}{10^8 M_\odot}\right)^{1/4}\left(\frac{\dot{m}}{0.01}\right)^{-1/4} \text{Å} \quad (6)$$

where r_2 is the location of the gap (in units of $r_g = GM_1/c^2$), M_1 is the mass of the primary SMBH, $\dot{m}$ is the Eddington accretion ratio ($\dot{m} = 1.0$ is the Eddington rate) and η is the accretion efficiency ($\eta = 0.06 - 0.42$ for the full range of black hole spins). Thus, a gap at $10^3 r_g$ in a thin homogeneous disk around a $10^6(10^8)M_\odot$ SMBH leads to a break at $\lambda_b \sim 0.4(1.4)(\eta/0.1)^{1/4}\mu$m. Eqn. 6 can be compared directly with eqn.(13) in (Gültekin & Miller 2012), with our pre-factor agreeing with theirs (~ 140) for $\eta \sim 0.1$ if their $f(w/h) \sim 0.6$. A sufficiently wide gap leads to a broad dip in the broadband optical continuum (see e.g. Fig. 1 in Gültekin & Miller (2012) for an illustration, although their break should be located around $\sim 2\mu$m not $\sim 0.2\mu$m). Local disk mass is expected to decrease rapidly at small radii, so we should observe deeper and wider spectral dips in the SED as λ_b decreases.

Assuming the irradiated outer disk flares, such that H/r is an increasing function of radius, the blackbody temperature of the irradiated outer gap wall ($T_{\rm wall}$) is given by (Armitage 2010)

$$T_{\rm wall} = L_{\rm inner}^{1/4}\theta^{1/4}r_{\rm wall}^{-1/2} \quad (7)$$

where $L_{\rm inner}$ is the AGN luminosity due to material at $r < r_{\rm wall}$ and $\theta = -H_r/r + dH_r/dr$ is the angle between the continuum source and the tangent to the disk surface and $H_r \sim H$ the disk thickness in the limit of a very optically thick disk. Rewriting in terms of $\dot{m}, M_1$ we find the peak wavelength of outer gap emission is

$$\lambda_{\rm wall} \approx 165\left(\frac{r_2}{r_g}\right)^{1/2}\left(\frac{M_1}{10^8 M_\odot}\right)^{1/4}\left(\frac{\dot{m}}{0.01}\right)^{-1/4}\theta^{-1/4}\text{Å} \quad (8)$$

where θ may be rewritten in terms of the opening angle of the disk at the wall (β) and radius of the inner accretion disk $r_{\rm in}$ as $\theta^{-1/4} \approx (cos\beta/4)^{1/4}(r_{\rm in}/r_{\rm wall})^{1/2}$. In a (more realistic) flared disk, λ_b due to the gap is found from the $r^{-1/2}$ dependence in eqn. 8 rather than the $r^{-3/4}$ dependence in eqn. 6. Thus, a gap at $10^3 \pm 10^2 r_g$ in a flared disk around a $10^6(10^8)M_\odot$ SMBH yields a break centered on $\lambda_b \sim 0.06(0.22)(\theta/30)^{-1/4}\mu$m and a corresponding bump due to the wall at $\lambda_{\rm wall} \sim 1.05 \times \lambda_b$.

In the gas pressure dominated region of the disk, the outer wall height can be approximated by (Armitage 2010)

$$H_{\rm wall} \approx \frac{c_s}{\omega} = \left(\frac{k_{\rm B}}{\mu m_p}\right)^{1/2} T_{\rm wall}^{1/2}\omega^{-1} \quad (9)$$

where c_s is the sound speed (see Kocsis et al. 2012b, for the radiation pressure dominated case). The maximum luminosity of the outer wall can be approximated by $L_{\rm wall,max} \approx (H_{\rm wall}/r)L_{\rm inner}/4$. Shadowing by the inner disk will reduce the observed value of $L_{\rm wall}$. For $H_{\rm wall}/r \sim 0.1$, then $L_{\rm wall} \leqslant 3\%L_{\rm inner}$.

In certain cases a cavity will form in the AGN disk rather than a gap. When the local disk mass $< M_2$, secondary migration will stall (e.g. Syer & Clarke 1995; Kocsis et al. 2012a; McKernan et al. 2013). As the inner disk drains 'inside-out', gas will pile-up at the outer gap edge and a cavity can form (McKernan et al. 2013). As the inner disk drains to form a cavity, $L_{\rm inner}$ decreases. Since our model predicts that in flared disks with gaps/cavities,

$$\lambda_{\rm wall} \approx 140\left(\frac{L_{\rm inner}}{10^{43}{\rm erg/s}}\right)^{-1/4}\left(\frac{\theta}{30}\right)^{-1/4}\left(\frac{r}{r_g}\right)^{1/2}\left(\frac{M_1}{10^8 M_\odot}\right)^{1/2}\text{Å} \quad (10)$$

for $L_{\rm inner} \sim 10^{42(43)}$ergs/s, $\lambda_{\rm wall} \sim 0.8(0.4)\mu$m at $10^3 r_g$. Our model predicts that while $L_{\rm inner}$ decreases, the SED slope at $\lambda \geqslant \lambda_{\rm wall}$ steepens due to continued viscous gas inflow and pile-up as $L_{\rm wall}$ increases. Thus, in disks with gaps/cavities, our model predicts an anti-correlation between average $L_{\rm inner}$ and the SED slope at $\lambda \geqslant \lambda_{\rm wall}$. This prediction distinguishes our model from models of cavity formation due to inner disk instability and collapse, since there is no (or little) pile-up in the latter case. Interestingly, pile-up at the outer gap edge will generate a luminous annulus in the disk, which may be detectable in an optical stellar transit of the AGN disk (see §6.1 below).

As the inner disk drains inside-out, regions of short timescale variability are removed from the AGN disk. Gas pile-up on the viscous timescale ($\tau_\alpha(r_{\rm wall})$) will be accompanied by disk drainage on much faster inner disk timescales. Thus, our model predicts that a decline in power on short timescales in the power density spectrum (PDS) of an AGN, due to removal of the inner disk, will be accompanied by a prominent peak in the PDS due to variation on the characteristic pile-up timescales. If we approximate the gas pile-up on the gap/cavity edge as an unstable, thick advective flow (particularly as photoionization declines), the timescale of variability ($\Delta t_{\rm wall}$) of such a flow is roughly the freefall timescale

$$\Delta t_{\rm wall} \geqslant 16\left(\frac{M_1}{10^8 M_\odot}\right)\left(\frac{r_{\rm wall}}{100 r_g}\right)^{3/2}\text{days} \quad (11)$$

which is comparable to observed prominent breaks on timescales of $\sim 5 - 100$ days in AGN PDSs (e.g. Collier & Peterson 2001). Even if the pile-up is unstable on short times and leaks completely into the gap/cavity, refilling the disk, torques from the secondary can still excavate a new gap/cavity in the disk and the cycle begins again.

The dam wall that holds back the piled-up gas may be leaky at best and not endure for long, particularly at high accretion rates (see McKernan et al. 2013, for extensive discussions). In the case of high accretion rates, cavities may be short lived and quickly refilled as stalled gap-opening migration resumes. Cavities will only persist until mass $\geqslant M_2$ builds up at the cavity edge, so the cavity lifetime is $\tau_{\rm cav} \geqslant M_2/\dot{M}_1$. The AGN disk lifetime is given by $\tau_{\rm disk} = q_{\rm disk}M_1/\dot{M}_1$, so among disks with IMBH, a fraction $\tau_{\rm cav}/\tau_{\rm disk} = q_2/q_{\rm disk}$ will exhibit cavities where $q_2 = M_2/M_1$ and $q_{\rm disk} = M_{\rm disk}/M_1$. Thus, if an AGN disk ($q_{\rm disk} \sim 10^{-2}$), hosts a sufficiently massive IMBH ($q_2 \sim 10^{-4}$) it has about a 1% chance of being observed with a cavity.

Disks around lower mass SMBH are the likeliest observational targets for finding gaps or cavities. Around low mass SMBH, note that even large mass (short-lived) stars could maintain a cavity in the inner disk for most of their main sequence lives. Around an SMBH with $M_1 = 10^6 M_\odot$, an AGN disk lasts $\tau_{\rm disk} \sim 50(q_{\rm disk}/10^{-2})(\eta/0.1)(M_6/10^6 M_\odot)(\dot{m}_1/0.01)^{-1}$Myr, where $\dot{m}_1$ is the Eddington ratio of the primary. A $M_2 = 10M_\odot$ stellar mass BH growing in this disk at $\dot{m}_2 \sim 3.5\times$Eddington via collisions and gas accretion reaches gap/cavity opening threshold

($q_2 \sim 10^{-4}, M_2 \sim 100 M_\odot$ in time $\tau_{\rm gap} \sim 35(\dot{m}_2/3.5)$Myr (McKernan et al. 2012). Assuming every low mass AGN disk starts off with a stellar mass black hole, if $\tau_{\rm gap} < \tau_{\rm disk}$, a crude estimate of the probability of a gap or cavity in disks around $M_1 \sim 10^6 M_\odot$ SMBH is $P_{\rm gap} = 1 - (\tau_{\rm gap}/\tau_{\rm disk})$ or

$$P_{\rm gap} = 1 - \left[0.7 \left(\frac{\dot{m}_2}{3.5}\right) \left(\frac{10^{-2}}{q_{\rm disk}}\right) \left(\frac{0.1}{\eta}\right) \left(\frac{10^6 M_\odot}{M_6}\right) \left(\frac{\dot{m}_1}{0.01}\right)\right]. \quad (12)$$

A more detailed estimate can be constructed by accounting for the location of M_2, the local mass supply and Bondi accretion (Kocsis et al. 2011; Ju et al. 2013). Thus, around low luminosity Seyfert AGN with $M_1 \sim 10^6 M_\odot$, we expect $\sim 1/3$ of disks to display evidence of gaps and only $\sim 1\%$ to display evidence for cavities. If IMBH in AGN disks start from stellar mass black hole seeds then only $\sim 1\%$ of higher luminosity Seyfert AGN will display evidence for gaps and little or no evidence for cavities due to IMBH formed in the disk. However, if IMBH survive the AGN phase, they can grow much larger in subsequent phases and a larger fraction of higher luminosity and higher mass AGN may display evidence for gaps and cavities. At $z < 0.1$, there are tens of well-studied X-ray selected Seyfert AGN including ~ 10 low mass Seyferts. Several of these AGN (e.g. MCG-6-30-15) are heavily absorbed in the optical/UV, so it is difficult to constrain optical accretion disks in these cases. A systematic survey of hundreds of optically selected AGN (e.g. from SDSS) will yield the strongest statistical constraints on the occurrence of gaps and cavities in AGN disks. If, after accounting for reddening and naturally occurring spectral breaks (e.g. Zheng et al. 1995), there is an absence of breaks in the 'big blue bump' of AGN SEDs, we can rule out the presence of close MBH mergers in AGN and severely restrict models of IMBH in AGN disks.

3.2 Predictions from a parallel with gapped protoplanetary disks

The previous section is based on physical expectations but we can also make predictions by analogy, based on observations of gapped protoplanetary disks. First, some emission lines in protoplanetary disks are observed to be double-peaked due to the presence of a gap or cavity, which leads to blue- and red-shifted peaks in the line emission (Andrews et al. 2011). By analogy, our model predicts double-peaked low ionization optical/UV line profiles in AGN. A small fraction of AGN are indeed observed to display double-peaked low-ionization emission lines (Strateva et al. 2003; Lewis, Eracleous & Storchi-Bergmann 2010). These lines and their variability (Lewis, Eracleous & Storchi-Bergmann 2010) can be accounted for by a gap-opening IMBH trailed and led by clumpy spiral density waves. Double-peaked lines observed in NGC 4151 for example, could be explained by a black hole binary, with a large mass secondary ($q \sim 0.01 - 0.1$) at large eccentricity (Bon et al. 2012). Our model predicts that double-peaked lines must originate outside the disk cavity, so a spectral break or dip in the SED must occur at $\lambda_b < \lambda_L$, the line wavelength. We can test this prediction in the sample of AGN with double-peaked lines, by comparing the timescales of variability of the double-peaked lines ($t_{\rm l}$) with the timescale of variability of the outer gap wall ($t_{\rm wall}$). If $t_{\rm l} \leqslant t_{\rm wall}$ then our interpretation of these lines must be incorrect.

Second, in protoplanetary disks, the outer gap/cavity wall is directly exposed to the stellar ionizing continuum and emits a blackbody at $\lambda_{\rm wall}$ with luminosity proportional to the wall height (Andrews et al. 2011), followed by a luminosity drop at $L(\lambda > \lambda_{\rm wall})$ due to shadowing by the wall. Our model predicts the same basic observable: a prominent blackbody peak in the AGN SED at $\lambda_{\rm wall}$, with $L(\lambda > \lambda_{\rm wall}) < L(\lambda_{\rm wall})$ due to shadowing. The luminosity at $\lambda_{\rm wall}$ varies on timescale $\Delta t_{\rm wall}$ which will be significantly faster than the timescale of variability at $\lambda > \lambda_{\rm wall}$.

Third, in the SEDs of gapped protoplanetary disks, as L($\lambda < \lambda_{\rm wall}$) increases, $L(\lambda > \lambda_{\rm wall})$ is observed to decrease, and vice versa (Espaillat et al. 2007). This 'see-saw' variability is believed to be due to occasional puffing up of the inner disk (short wavelengths), shadowing the outer disk wall (long wavelengths). By analogy, our model predicts exactly this sort of spectral variability in gapped AGN disks. We predict that during a flaring high state in X-rays from the innermost disk, $L(\lambda < \lambda_{\rm wall})$ due to the irradiated inner disk must increase. Since the puffed up inner disk shadows the outer gap, $L(\lambda_{\rm wall})$ must decrease. Conversely, during an AGN 'low state' where L_x diminishes, $L(\lambda < \lambda_{\rm wall})$ will also decrease, but $L(\lambda_{\rm wall})$ must increase as the outer gap/cavity wall is no longer shadowed by the puffed-up inner disk. Thus, in sources that are X-ray luminous (i.e. with a substantial inner disk), but with high flaring or low states, our model predicts a linear correlation between L_x and $L(\lambda < \lambda_{\rm wall})$, but an anti-correlation between L_x and $L(\lambda_{\rm wall})$.

3.3 LINERs as AGN disks with cavities

A sub-class of galactic nuclei, LINERs, do not exhibit a prominent blue/UV bump in their SEDs (e.g. Maoz et al. 2005; Ho 2008). Thus either LINERs do not have a prominent thermal disk or the accretion flow is radiatively inefficient. If there is no accretion disk, photoionization could be powered by AGB stars (e.g. Eracleous et al. 2010). We suggest an alternative possibility. In our model, a substantial cavity carved out by an IMBH (or SMBH), can account for the absence of a prominent disk signature. By removing the inner disk to large radii, the reduced ionizing continuum luminosity will change the optical line ratio from AGN-like. If the massive binary in the cavity is accreting weakly due to a leaky dam (see Sec. 2), the ionizing continuum will have a much lower luminosity, akin to LLAGN or an ultra-luminous X-ray source (ULX) and therefore the observed line ratios must be LINER-like (McKernan et al. 2011b). ULXs (which may be powered by accretion onto IMBH) have now been observed with optical line ratios remarkably consistent with those in LINERs and LLAGN (Berghea & Dudik 2012). Thus, our model predicts that many LINERs consist of MBH binaries in large central cavities in a gas disk. A small fraction of these LINERs will be GW loud (depending on $a_{\rm bin}$).

Specifically our model predicts: (1) a rise in the optical spectrum of LINERs due to the cavity wall at $\lambda_{\rm wall}$, together with (2) an immediate dip at $\lambda > \lambda_{\rm wall}$ due to pile-up and disk shadowing of a weakly accreting central source, (3) significantly shorter variability timescales at $L(\lambda_{\rm wall})$ compared to $L(\lambda > \lambda_{\rm wall})$, (4) little or no power in the LINER PDS on timescales $< t_{\rm wall}$ and (5) double-peaked low ionization lines at $\lambda > \lambda_{\rm wall}$. In this model, the IMBH/SMBH occupy a substantial cavity. If the cavity is not leaky the binary will not accrete strongly. Such LINERs will not exhibit a prominent, luminous, soft X-ray excess (see §5 below). However, if the cavity is leaky, accretion onto the IMBH/secondary MBH could dominate the accretion onto the SMBH yielding ULX-like optical line ratios.

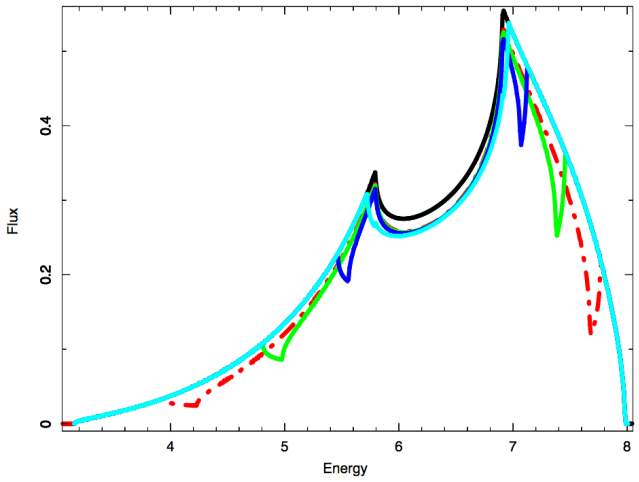

Figure 1. The change in Fe Kα profile for the in-migration of a $q = 3 \times 10^{-3}$ IMBH across the inner disk with empty gap of width $2R_H$ where $R_H = (q/3)^{1/3}R$. Flux is in normalized arbitrary units and Energy is in units of keV. Solid black line indicates the unperturbed Fe Kα profile. Turquoise solid line denotes an annulus at $90 \pm 9r_g$ in the inner disk. Dark blue solid line denotes an annulus at $50 \pm 5r_g$, Green solid line corresponds to an annulus at $20 \pm 2r_g$ and the dashed red line corresponds to an annulus at $10 \pm 1r_g$. See McKernan et al. (2013) for detailed discussion of this and other effects in the broad FeKα line as well as detectability with future missions.

4 GAPS & CAVITIES IN INNER AGN DISKS: PREDICTIONS

In the limit of small disk radii, as a gap-opening IMBH migrates closer to the supermassive black hole, the gap in the accretion disk can imprint itself on the broad component of the Fe Kα line profile (see McKernan et al. 2013, for extensive discussion). Fig. 1 illustrates the simulated, noiseless variation in a broad Fe Kα line profile due to an in-migrating empty annulus (occupied by an IMBH) of width $2R_H$ (where $R_H = (q/3)^{1/3}a$) and a is the circularized orbit radius) decreasing from $100r_g$ to $6r_g$. We calculated the broad Fe Kα line profile around a Schwarzschild black hole using the `diskline` algorithm Fabian et al. (1989). We assumed $q = 3 \times 10^{-3}$, the disk is inclined by 60^o to the observer's line of sight and the X-ray continuum goes as $r^{-2.5}$. As the IMBH and gap migrate into the inner $100r_g$ of the disk, a flux deficit appears (turquoise solid line) compared to the unperturbed profile (black solid line). As inward migration continues, the empty gap removes flux from increasingly red and blue regions of the disk and the twin notches move apart, red-ward and blue-ward respectively from the line center (6.4keV). As the empty gap moves inwards in the disk from $50r_g$ to $10r_g$ (red curve), the blue notch moves from 6.5keV out to 7.2keV, and the red notch moves from 5.6keV to 4.2keV.

The timescale to merger of an IMBH-SMBH binary via gravitational radiation is given by (Peters 1964)

$$\tau_{\rm GW} \approx 10^{12}{\rm yr} \left(\frac{10^3{\rm M}_\odot}{\rm M_2}\right) \left(\frac{10^6{\rm M}_\odot}{\rm M_1}\right)^2 \left(\frac{\rm a_{bin}}{0.001{\rm pc}}\right)^4 (1-{\rm e}^2)^{7/2} \quad (13)$$

where M_2 is the mass of the secondary IMBH, M_1 is the mass of the primary supermassive black hole, $a_{\rm bin}$ is the binary separation and e is the IMBH orbital eccentricity. For a $3000M_\odot$ IMBH around a $10^6 M_\odot$ supermassive black hole, the progression from green to red curve in Fig. 1 takes $\sim$ 16yrs and from red curve to final merger takes $\sim$ 1yr. Low mass AGN exhibiting broad Fe Kα lines (e.g. MCG-6-30-15) have the shortest timescales for merger and low mass migrators (IMBH and stellar mass BH) in the inner disk are the most likely sources of a late-stage ripple effect (McKernan et al. 2013). Oscillations caused by e.g. an accreting secondary (IMBH) in a cavity around a primary SMBH can be readily tested with the proposed *LOFT* mission (see McKernan et al. (2013) for further details). Future X-ray missions such as *Astro-H* and *IXO-Athena* have the energy resolution to distinguish between features due to highly ionized Fe (e.g McKernan & Yaqoob 2004) and may detect the ripple signatures or oscillations. Observations of the latter stages of the ripple effect in the broad FeKα line of a low mass AGN, predict a prompt rise in gravitational wave (GW) luminosity from this source, which should reach the threshold of future GW detectors. This signal therefore constitutes a prime EM precursor for GW observations.

5 EMBEDDED OBJECTS IN AGN DISKS: PREDICTIONS

In this section, we discuss the case of embedded objects in AGN disks, including IMBH that do not open a gap. In §5.1 we discuss the observational signatures of accreting embedded objects in the AGN disk. In §5.2 we discuss observational signatures due to embedded objects on retrograde orbits within the AGN disk. In §5.3 we examine whether one or other or both models could contribute to, or correspond wholly to the soft X-ray excess observed in many AGN.

5.1 Predictions from accretion

IMBH can accrete from the gas disk at up to Eddington rates (Nayakshin & Sunyaev 2007), although they can grow at super-Eddington rates including collisions in the disk (McKernan et al. 2013). A gas disk accreting onto an IMBH produces a blackbody spectrum peaking in the soft X-ray band at temperatures of $\sim 0.1{\rm keV}(10^4{\rm M}_\odot) - 1{\rm keV}(10^2 M_\odot)$. This is observationally interesting because in many (possibly most) AGN, an excess of soft X-rays ($\sim 0.1 - 1.0$keV) is observed, relative to the level expected from extrapolating a powerlaw fit from hard X-rays (> 1keV) (e.g. Gierliński & Done 2004; Scott et al. 2012). The excess is observed to have a quite remarkable constant temperature peak, independent of large variations in observed AGN luminosity (Crummy et al. 2006; Winter et al. 2012). The origins of the soft excess remain unknown, however accretion onto an IMBH (or population of IMBH seeds) in the AGN disks could account for the luminosity and energy of the soft excess (McKernan et al. 2010b, 2011b).

From §3, the innermost disk blackbody temperature for a thin disk around an IMBH of mass M_2, is $T \propto M_2^{-1/4}$, with luminosity $L \sim \eta \dot{M}_2 c^2$, where η is the accretion efficiency. For black holes $(10 - 10^4 M_\odot)$, $T \sim 10^7 - 10^6$K (or $\sim 1 - 0.1$keV) and $L \sim \eta 10^{39} - 10^{42} \dot{m}_{\rm Edd}$ ergs^{-1}, where $\dot{m}_{\rm Edd}$ is the Eddington ratio. The soft X-ray excess in AGN peaks at ~ 0.1keV with $L_{sx} \sim 10^{42-43}$ erg s^{-1} (e.g. Reynolds 1997; Winter et al. 2012). Thus, accretion onto IMBH with masses $\geqslant 10^4 M_\odot$ could account for the observed soft excess in AGN. In this model L_{sx} increases as a function of $M_2, \dot{M}_2$, since from eqn. 6 $T_{sx} \propto M_2^{1/4} \dot{M}_2^{1/4}$. Once an IMBH grows massive enough to open a gap ($q_2 \geqslant 10^{-4}$, depending on $H/r, \alpha$), we expect L_{sx} to drop dramatically, unless the IMBH has an eccentric orbit (Roedig et al. 2012). In this model, AGN without a significant soft excess harbour gap-opening IMBH or very low mass IMBH.

The building blocks of IMBH in our model (nuclear cluster

objects) will also accrete and generate (potentially) observable signatures. Some 10^4 white dwarfs accreting at Eddington could produce a soft X-ray spectral bump $\sim 0.03-0.05$keV (van den Heuvel et al. 1992) with luminosities $\sim 10^{42}$ erg s^{-1}. Stars embedded in the AGN disk will look similar to T-Tauri stars, emitting X-rays at $\sim 10^7$K (~ 0.9keV) but L_x is only $\sim 10^{28} - 10^{32}$ergs^{-1} (Preibisch et al. 2005). So, even a large population ($\sim 10^5$) of T-Tauri stars in the disk would be insufficient to reproduce the AGN soft X-ray excess luminosity and a large fraction of the T-Tauri luminosity will be reprocessed as IR.

5.2 Predictions for objects on retrograde orbits

Unlike protoplanetary disks, nuclear cluster objects (NCOs, i.e. stellar mass black holes, stars, stellar remnants) in AGN disks can follow retrograde orbits. Migration onto the SMBH will only occur if the retrograde NCO captures 'negative' angular momentum within its influence radius from a comparable mass of gas (e.g. Nixon et al. 2011). If most gas flows past the NCO, very little negative angular momentum will be transferred. Large-mass retrograde NCOs embedded in a disk (not in a cavity as in Nixon et al. (2011)) will not open gaps because of lack of retrograde resonant torques. However, they may open a narrow annular gap as wide as their Bondi radius. Retrograde NCOs and IMBHs could persist a long time at the same AGN disk radius due to far weaker torques than predicted by standard Type I and Type II migration scenarios (calculated for prograde orbiters). The observational signature of retrograde objects will be the X-ray generating bow shock associated with the headwind of NCO retrograde motion.

Fig. 2 shows the results of a 2-d simulation using the PENCIL CODE [1] of a satellite with mass ratio $q = 10^{-4}$ on a retrograde orbit in an isothermal, constant temperature disk of aspect ratio $H = 0.05$ in a box of dimensions $r = [0.4, 2.0], \phi = [-\pi, \pi]$. From Fig. 2 the tapering spiral density waves we would expect to see in the prograde case are replaced with equal (but very small) magnitude density waves. Since the material in the tail increases by $\leqslant 2\%$ only over background after 42 orbits, the net torque of the gas on the retrograde NCO is far smaller than in standard (Type I or II) migration scenarios, so the NCO remains at approximately the same disk radius. A bow shock caused by a star passing through a disk at relative velocity v_r will heat gas behind the shock to $T \sim 0.1 m_p v_r^2/k$ (Zentsova 1983), where m_p is the proton mass and k is Boltzmann's constant. To generate bow shocks with temperatures $\sim 0.1 - 1$keV, requires relative velocities in the range $v_s \sim 300 - 1000$kms^{-1}, implying retrograde NCOs on Keplerian orbits in the outermost disk or torus ($\sim 10^{4-5} r_g$). The associated shock luminosity $L \approx \sigma A T^4 \sim 10^{42-43}$ erg/s requires the area of ~ 20 Sun-like stars on retrograde orbits. Alternatively, the shock luminosity could be due to the single collision cross-section ($\sigma_{\rm coll} \approx \pi r_g^2 (1 + 4GM_2/r_g v_s)$) of a $M_2 \sim 10^{3-4} M_\odot$ IMBH on a retrograde orbit in the outer disk. This model of the soft X-ray excess predicts little fractional variability in the soft excess as well as a constant soft excess luminosity, independent of changes in the continuum due to accretion onto the primary SMBH. This model can be ruled out if the luminosity and variability of the soft excess and the X-ray continuum are correlated, which can be tested for a large sample of nearby AGN with *LOFT*.

[1] The code is publicly available under a GNU open source license and can be downloaded at http://pencil-code.googlecode.com

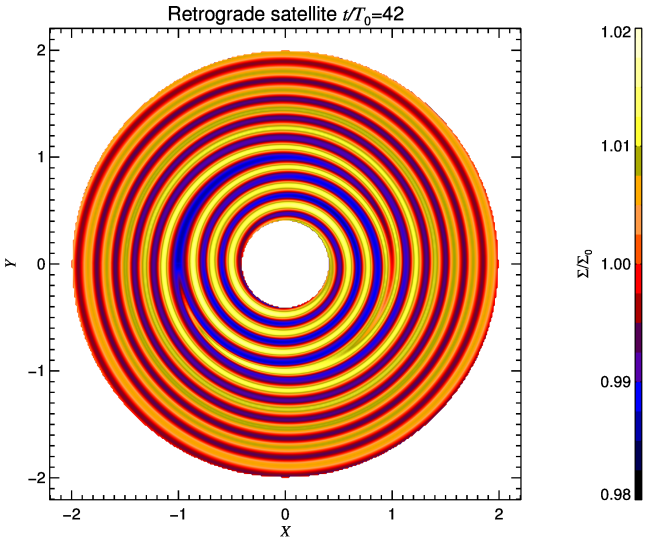

Figure 2. A 2-d simulation of an NCO with mass ratio $q = 10^{-4}$ on a retrograde orbit in an isothermal, constant temperature disk of aspect ratio $H = 0.05$ in a box of dimensions $r = [0.4, 2.0], \phi = [-\pi, \pi]$. An identical prograde orbiter in the same disk, after the same time, opens a prominent gap and generates spiral density waves an order of magnitude larger than those here, leading to standard Type II migration.

5.3 Comparison with observations

The Swift Burst Alert Telescope (BAT) in the 14-195keV band is unbiased towards obscured sources and host galaxy properties (e.g. Winter et al. 2012). Fig. 3 shows those AGN from the BAT sample that require a soft X-ray excess fit to the continuum (Winter et al. 2012). As we can see, the result is a scatterplot, but centered around ~ 0.1keV. The two dashed-dotted lines in Fig. 3 correspond to our two simple models of the soft excess. The horizontal dotted line corresponds to X-ray emission due to bow shocks centered on a constant velocity of ~ 100 km s^{-1} in the outer AGN disk, due to NCOs and IMBH on retrograde orbits. The sloping dashed line corresponds to the gap-opening threshold for an IMBH ($q \leqslant 2 \times 10^{-4}$, for fiducial disk parameters of $H/r \sim 0.05, \alpha \sim 0.01$) as a function of primary SMBH mass. There is substantial scatter around both model fits, but the constant temperature model is a better global fit (confirmed by a simple χ^2 test). The IMBH accretion model predicts weak or no emission from IMBH below the sloped dashed line because such objects should open a gap and decrease accretion. However, we cannot rule out this model based on Fig. 3 alone since a small factor of $\sim 2 - 3$ on H/r and α, particularly in disks around lower mass SMBH, could account for soft excesses below the sloped dashed line. The retrograde orbits model can account for the range of 43/45 of the AGN in Fig. 3 if the 'median headwind' simply lies in the range $30 - 300$ km s^{-1} (implying most NCOs/IMBH are $> 10^3 r_g$ from the SMBH). In order to rule out one or both models, we need constraints from variability studies, using large effective area X-ray telescopes such as the future *LOFT* mission.

5.3.1 *Test cases: Ton S180 & future suggestions*

Constraining models of the soft excess is complicated by the presence of warm absorbing gas in AGN (McKernan et al. 2007). In order to distinguish between models of the soft excess, it helps to consider AGN with a soft excess but little or no warm absorption.

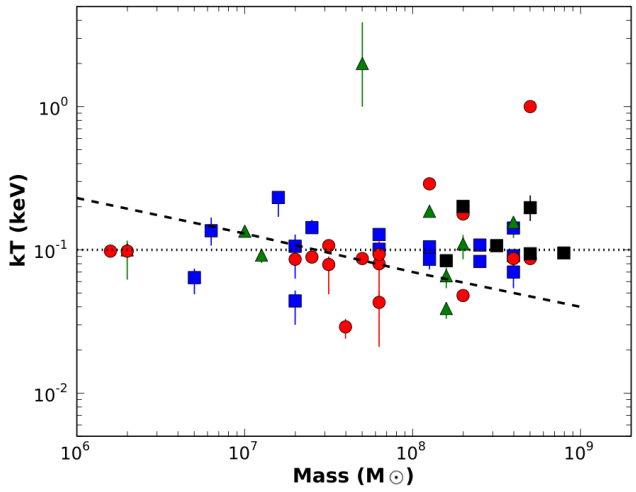

Figure 3. The peak energy (kT) of the soft X-ray excess found in AGN observed with Swift-BAT plotted against the mass of the central supermassive black hole (from Winter et al. (2012)). Blue squares are Seyfert 1s, black squares are broad line radio galaxies, green triangles are Seyfert 1.2s and red circles are Seyfert 1.5s. The horizontal dotted line corresponds to a model of $\sim$ 0.1keV thermal emission due to bow-shocks from NCOs/IMBH on retrograde orbits in the AGN disk, encountering 'headwinds' centered on 100 km s^{-1}. The sloping dashed line corresponds to IMBH with a constant mass ratio $q = 2 \times 10^{-4}$. Below this line, in AGN disks with fiducial $H/r = 0.05, \alpha = 0.01$ we expect no soft excess due to accreting IMBH (see text).

For example, the narrow line Seyfert galaxy Ton S180 (Veron-Cetty & Veron 2006) in a low state reveals a substantially stronger fractional variability in the softer X-rays than in hard X-rays (Nardini et al. 2012). In high states, the fractional variability of soft X-rays in Ton S180 appears to be similar to that of hard X-rays. In this AGN, we can rule out objects on retrograde orbits as a cause of the soft X-ray excess. If the soft excess is due to IMBH accretion, it evidently dominates emission during the low state while continuum emission dominates during the high state. However, rather than investigating individual idiosyncratic sources, it makes more sense to study a sample of AGN with soft excesses, but no warm absorption, particularly during low X-ray states where the continuum does not dominate. Observations of such a sample of AGN during 'low' states, with the large collecting area of *XMM* or future missions such as *LOFT*, will allow us to test the IMBH accretion model by comparing the variability timescales of the soft excess and the hard X-ray continuum. The accreting IMBH model predicts that the ratio of soft excess/continuum variability timescales during the low state is a function of the mass ratio (q) of the IMBH to the supermassive black hole. On one hand, competing models of the soft excess emission, such as blurred reflection (Crummy et al. 2006) can be ruled out if it can be shown that the soft excess consistently varies on shorter timescales than the continuum. On the other hand, we can rule out the presence of luminous, accreting IMBH in AGN disks if the fractional variability of the soft excess and the hard powerlaw components are identical for a large sample of these AGN in 'low' X-ray states.

6 INTERMITTENT IMBH SPECTRAL SIGNATURES:PREDICTIONS

Once-off (or intermittent) observational signatures of IMBH in AGN disks or (more likely) in post-AGN galactic nuclei will be observed infrequently, but can provide strong evidence for the presence of an IMBH in a galactic nucleus. From eqn. 13, a $10^2 M_\odot$ IMBH will remain orbiting a $10^6 M_\odot$ SMBH for $\sim$Gyr if located $\geqslant 2000 r_g$. IMBH may survive the AGN phase, in the same way that Jupiter-sized planets survive protoplanetary disks. Therefore we should expect to find IMBH in quiescent galactic nuclei (with enhanced stellar tidal disruption rates) and such IMBH may act as seeds for further growth in a new AGN phase. If IMBH are common in AGN disks (as we propose), surveys of hundreds of nearby galactic nuclei using e.g. LSST in the optical band will find the occasional event as described below.

6.1 Transits of AGN disks:predictions

An accreting IMBH in an AGN disk produces an asymmetric X-ray intensity distribution. The asymmetry of the X-ray intensity distribution may be detectable by a transit of a bloated star or optically thick cloud across the face of an AGN (see Béky & Kocsis 2012, for detailed transit calculations). The first such transit in an AGN was observed in MCG-6-30-15 (McKernan & Yaqoob 1998). This was followed by observations of transits in among others: NGC 3516 (Turner et al. 2008), NGC 1365 (Maiolino et al. 2010) and Cen A (Rivers et al. 2011). A transit event, though rare, gives us a chance to map the AGN continuum at unprecedented resolution ($<$ microarcseconds). If the X-ray intensity profile is asymmetric, this will show up in the best-fit to the transit profile (McKernan & Yaqoob 1998). A systematic archival search of AGN X-ray lightcurves for transit profiles (a significant task far beyond the scope of this paper), will map the innermost accretion disk at unprecedented angular resolution and put strong limits on the occurrence of IMBH in AGN inner disks. In the optical band, transits can reveal rings of enhanced emission due to the pile-up of gas outside the orbit of a gap- or cavity-opening IMBH.

6.2 QPOs and spiral density waves

Quasi-periodic oscillations are occasionally observed in AGN and a fascinating possibility is that they arise due to the action of spiral density waves in the AGN disk (Czerny et al. 2010). Depending on the disk structure, migrating IMBH should have particularly strong associated spiral density waves, analagous to those associated with migrating giant planets in protoplanetary disks (Armitage 2010). For example, a 3-4ks QPO is observed in RE J1034 + 396 enhancing the flux by $\sim 5 - 10\%$ in the 0.3-10keV X-ray band Czerny et al. (2010). The orbital time at $\sim 6 r_g$ around a $10^7 M_\odot$ SMBH is $\sim$ 3ks. For a $10^5 M_\odot$ gas disk around a $M_1 = 10^7 M_\odot$ SMBH we expect $\leqslant 1\%$ or $\sim 10^3 M_\odot$ of gas within $10^2 r_g$ from a standard thin disk model (Sirko & Goodman 2003). If this QPO is due to spiral arms from a migrating IMBH in the AGN disk, the IMBH is $M_2 \leqslant 10^3 M_\odot$ and $a_{\rm bin} \sim 10^2 r_g$ from the SMBH. The IMBH will merge with the SMBH within $\sim 60 (10^3 M_\odot/M_2)(10^7 M_\odot/M_1)^2 (a_{\rm bin}/10^2 r_g)^4$kyrs. Since the co-rotating mass of gas at $r < 10^2 r_g$ is small, the IMBH will open a gap in the inner disk. RE J1034 + 396 is therefore a prime candidate for follow-up study of the broad component of the Fe Kα line (see §4 above). Post-merger, we also expect a kick on the merged

object to generate a density caustic that ripples outward in a spiral wave that decays with time, but only for mass ratios $q > 10^{-2}$ (Haiman et al. 2008). A future timing mission like LOFT is needed in order to do a high cadence variability study of a large sample of nearby X-ray bright AGN. Spiral density waves raised by a migrating IMBH may show up as ripples in the broad FeKα line profile. Future timing studies of broad FeKα lines with the energy resolution and effective area of *Athena* will help constrain the location of IMBH migrators in AGN disks.

7 GRAVITATIONAL WAVES: PREDICTIONS

Our model predicts a large number of merging nuclear cluster objects (NCOs) and IMBH in the accretion disk around a SMBH which may be rich sources of gravitational waves (GWs). A binary emits GWs with characteristic GW frequency (Peters & Mathews 1963)

$$f_{\rm GW} \sim \frac{(1+e)^{1/2}}{(1-e)^{3/2}} \sqrt{\frac{GM}{a^3}}\,. \quad (14)$$

The detectable GW frequency band of the planned spaced-based GW observatory LISA[2] or NGO[3] (Amaro-Seoane et al. 2011) is between 10^{-4} and 1 Hz, and between 10 to 3000 Hz for the existing Earth-based instruments LIGO[4] and VIRGO[5]. Binaries orbiting outside the last stable orbit, $a(1-e^2) \gtrsim (6+2e)\ r_g$, are in the LISA (LIGO) frequency band if the total mass $M = m_1 + m_2$ is between 10^3–$10^7\ M_\odot$ (1–$10^3\ M_\odot$). We discuss the GW signatures of various mass sources in turn below.

7.1 GWs from an IMBH orbiting a SMBH

A compact object orbiting around a SMBH on a circular orbit emits GWs in the LISA band if the orbital period is less than 6 hours. For SMBH mass $10^6\ M_\odot$ ($10^7\ M_\odot$), this corresponds to an orbital radius less than $75\ r_g$ ($16\ r_g$), or a time to merger less than 100 yr (20 yr) for an IMBH $\mu = 10^3\ M_\odot$. The signal to noise ratio (SNR) decreases with source distance and increases with μ as $S/N \propto \mu/D$. The detectable distace of a circular SMBH–IMBH binary with $S/N = 10$ with LISA is very roughly[6]

$$D_{\rm LISA} \sim 1\,{\rm Gpc} \left(\frac{M}{10^6 M_\odot}\right)^{-2} \frac{\mu}{10^3 M_\odot} \left(\frac{r}{30\,r_g}\right)^{-4} \left(\frac{T}{1\,{\rm yr}}\right)^{1/2} \quad (15)$$

where T is the observation time. Eqn. 15 implies we will detect all SMBH-IMBH mergers out to $z \sim 0.3$. The GW phase evolution may be used to independently detect and distinguish thousands of SMBH–IMBH binaries in the Universe with LISA, if they exist. The binary separation shrinks over timescale $\tau_{\rm GW} \propto r^4$ given by Eq. (13). The relative fraction of SMBH-IMBH binaries in the Universe, that reside in a logarithmic separation interval centered at r, is proportional to $\tau_{\rm GW}$ (Eqn. (13)). Thus, most binaries will reside at large separations. However, the SNR increases toward smaller separations as r^{-4}, which implies that LISA will discover SMBH–IMBH binaries with a uniform probability distribution as a function of $\ln(r)$. However, at very small frequencies, the sources may constitute an unresolved GW background of $100 M_\odot$ intermediate mass ratio inspirals (see Barack & Cutler 2004b, for extreme mass ratio inspirals).

Once LISA detects a SMBH–IMBH binary, it can measure its physical parameters from the GW signal including the masses, separation, eccentricity, sky location, and distance to the source to a level similar to SMBH-SMBH mergers. The sky localization precision is of order $1\ {\rm deg}^2$ for a SMBH-SMBH or SMBH-NCO binary approaching merger ($r \lesssim 10 r_g$) at cosmological redshift $z = 1$ (Barack & Cutler 2004a; Lang et al. 2011; Mikóczi et al. 2012), and $10\ {\rm deg}$ or more at separations $r \gtrsim 20\,r_g$ (Lang & Hughes 2008; Kocsis et al. 2007). If the SMBH-IMBH inspirals can be identified with a similar accuracy, the 3D source localization accuracy may be sufficient to identify a unique AGN or LINER counterpart to the GW source approaching merger (Kocsis et al. 2006a). If not it will provide a $10\ {\rm deg}^2$ sky area for a deep triggered search for other electromagnetic signatures days to months before merger (see Kocsis et al. 2007, 2008). Bright AGN activity is not expected during merger if the torques of the secondary excavates a hollow cavity in the disk; instead we expect LINER-like activity (see §3.3 above). However, depending on the 'leakiness' of the cavity wall, non-axisymmetric streams can supply gas to the inner regions, leading to a coincident electromagnetic counterpart (see discussion in §2). A precise measurement of the GW phase may also be used to look for perturbations caused by the astrophysical environment around the SMBH–IMBH binary. The LISA measurement accuracy is sufficient to detect the torques generated by the spiral density waves in the accretion disk if $\mu \lesssim 100 M_\odot$ (Kocsis et al. 2011; Yunes et al. 2011).

7.2 NCOs-IMBH & IMBH-IMBH mergers

In our model the accretion disk is expected to host abundant stellar-mass NCOs. Upon close encounters with the IMBH, these objects may become bound to the IMBH on very eccentric orbits due to GW emission (O'Leary et al. 2009). Thus, our model *predicts a new, unexpected source of GWs*. These systems generate repeated GW bursts, detectable with both LIGO and LISA coincidentally (Kocsis & Levin 2012). This is possible if the orbital time is less than $6\ {\rm h}$ for LISA detections, and the pericenter passage timescale less than a $0.1\ {\rm s}$ for LIGO detections. As the eccentricity shrinks, the signal morphs into a continuous inspiral signal, and eventually a merger and ringdown. The detection range for LIGO and LISA is between 1–10 Gpc and 10 Mpc, respectively (East et al. 2013), so the odds of a coincident detection are remote.

There are no studies on the parameter estimation accuracy of repeated burst sources to date. Arguably, it should be much better than for circular sources, since these sources are in the detectable frequency band for a much longer time, the signal power is enhanced at large frequencies due to eccentricity, and these sources exhibit apsidal precession which can break parameter degeneracies (Mikóczi et al. 2012). For circular sources IMBH–NCO binaries are outside the detectable range of existing Earth-based observatories. Their detection requires the future third generation instrument,

[2] http://lisa.nasa.gov/
[3] http://elisa-ngo.org/
[4] http://www.ligo.caltech.edu/
[5] http://www.ego-gw.it/
[6] Here we assume that the LISA detector noise spectral amplitude decreases approximately as f^{-2} for $f \lesssim 10^{-3}$Hz (Barack & Cutler 2004a), and used that the dimensionless GW strain amplitude scales as $h \propto G^2 c^{-4} M\mu/(rD)$, according to the leading order quadrupolar radiation formula averaged over binary orientation. $D_{\rm LISA}$ varies by a factor 10 for $f \lesssim 10^{-2}$ Hz due to the unresolved white dwarf background and different orientations.

the Einstein Telescope[7]. With the latter, circular IMBH–NCO binaries may be localized within 2 deg accuracy for $S/N = 30$, the mass and distance measurement errors are 0.1% and 10% respectively (Huerta & Gair 2011).

Interestingly, the GW signal of IMBH–NCO binaries may carry information on the SMBH as well. First, the GWs are modulated by Doppler shift as the binary orbits around the SMBH (Yunes et al. 2011). Furthermore, the SMBH can secularly excite the eccentricity of the IMBH–NCO binary(Antonini & Perets 2012; Naoz et al. 2012). Since the GW signal is extremely sensitive to eccentricity (Peters & Mathews 1963), it is likely that this perturbation would allow us to constrain the parameters of the central SMBH. This effect is the inverse of that mentioned at the end of Section 7.1. LIGO or the Einstein Telescope may measure the SMBH through its influence on the IMBH-NCO system, while LISA may measure the effects of an NCO through the pertubations of the SMBH–IMBH signal.

7.3 NCO–NCO scattering and capture

Finally, the NCOs which form or become captured by the accretion disk may undergo close encounters and form hard binary systems through GW emission. Hard binaries are likely IMBH seeds in AGN disks (see Paper I). For these systems, the GWs are detectable with LIGO during pericenter passage (Kocsis et al. 2006b; O'Leary et al. 2009; Kocsis & Levin 2012; Samsing et al. 2013; East et al. 2013). Similar to the IMBH–NCO case, the signal initially consists of repeated bursts, but transitions to a continuous eccentric inspiral in a much shorter time of minutes to days depending on the impact parameter (see Eq. 13 with $\mu \sim M \sim 10\,M_\odot$).

These sources are in the LIGO frequency band before merger even in the circular case. For circular NS–NS inspirals, the source localization of the LIGO–VIRGO network is very poor 50 deg or more for $S/N \sim 15$, but it improves to within than 10 deg with future extensions of the network through KAGRA[8] or LIGO-India[9] (Nissanke et al. 2010, 2011; Veitch et al. 2012). Similar to the IMBH–NCO case, the source localization for eccentric sources is expected to be much better. The pertubations caused by the IMBH and the SMBH may be detectable. Remarkably, NS/BH and NS/NS binaries may have coincident electromagnetic counterparts, i.e. short-hard gamma ray bursts. The coincidence in time of an electromagnetic signal like a gamma-ray burst or the FeKα ripple effect allows us to locate the likely GW source.

8 CONCLUSIONS

If Intermediate mass black holes (IMBHs) can grow efficiently in AGN disks, the AGN host should exhibit myriad observational signatures. IMBHs that open gaps in AGN disks will exhibit strong observational parallels with gapped protoplanetary disks and may be detectable near merger in the broad FeKα line. LINER activity may be due to a weakly accreting MBH binary in a large disk cavity. If IMBHs do not open a gap, detection depends on signatures of accretion onto the IMBH (including tidal disruption events). We summarize observational signatures and compare them to current data where possible or suggest future observations.

[7] http://www.et-gw.eu/
[8] http://gw.icrr.u-tokyo.ac.jp/lcgt/
[9] http://www.gw-indigo.org/tiki-index.php?page=LIGO-India

ACKNOWLEDGEMENTS

We thank the referee for a report that helped us condense and focus this paper. We acknowledge very useful discussions with Tahir Yaqoob, Stephan Rosswog, Zoltan Haiman, Ari Laor, Hagai Perets, Kayhan Gültekin and Mordecai Mac Low. BM and KESF acknowledge support from NASA-APRA08-0117 and NSF PAARE AST-1153335. BK was supported in part by the W.M. Keck Foundation Fund of the Institute for Advanced Study and NASA grant NNX11AF29G. WL acknowledges support by the National Science Foundation under grant No. AST10-09802. This work was performed in part under contract with the California Institute of Technology (Caltech) funded by NASA through the Sagan Fellowship Program executed by the NASA Exoplanet Science Institute.

REFERENCES

Alexander T. 2005, Phys. Rep., 419, 65
Alexander T. 2007, astro-ph/0708.0688
Amaro-Seoane P. et al. 2012, CQG, 29, 124016
Amin M.A. & Frolov A.V. 2006, MNRAS, 370, 42
Andrews S.M., Wilner D.J., Espaillat C., Hughes A.M., Dullemond C.P., McClure M.K., Qi C. & Brown J.M., 2011, ApJ, 732, 42
Antonini F. & Perets H. 2012, ApJ, 757, 27
Armitage P.J. & Natarajan P., 2002, ApJ, 567, L9
Armitage P.J., 2010, Astrophysics of Planet Formation, Cambridge University Press
Artymowicz P. & Lubow S.H., 1996, ApJ, 467, L77
Barack L., & Cutler C. 2004a, PRD, 69, 082005
Barack L., & Cutler C. 2004b, PRD, 70, 122002
Baruteau C., Ramirez-Ruiz E. & Masset F., 2012, MNRAS, 423, 65
Béky B. & Kocsis B., 2013, ApJ, 762, 35
Berghea C.T. & Dudik R.P., 2012, ApJ, 751, 104
Bon E. et al., 2012, ApJ, 759, 118
Brown W., Geller M.J. & Kenyon S.J., 2012, ApJ, 751, 55
Bryden G., Chen X., Lin D.N.C., Nelson R.P., Papaloizou J.C.B., 1999, ApJ, 514, 344
Chang P., Strubbe L.E., Menou K. & Quataert E. 2010, MNRAS, 407, 2007
Collier S. & Peterson B.M. 2001, ApJ, 555, 775
Crummy J., Fabian A.C., Gallo L. & Ross R.R. 2006, MNRAS, 365, 1067
Crida A., Morbidelli A. & Masset F. 2006, Icarus, 181, 587
Czerny B., Lachowicz P., Dovciak M., Karas V., Pechacek T. & Das Tapas K. 2010, A&A, 524, A26
Davis S.W., Narayan R., Zhu Y., Barret D., Farrell S.A., Godet O., Servillat M. & Webb N.A. 2011, ApJ, 734, 111
D'Orazio D.J., Haiman Z., MacFadyen A., MNRAS, submitted, arXiv:1210.0536
East W.E., McWilliams S.T., Levin J. & Pretorius F., 2013, PhRvD, 87, 3004
Edgar R.G., Quillen A.C. & Park J., 2007, MNRAS, 381, 1280
Eracleous M., Hwang J.A., Flohic H.M.L.G., 2010, ApJ, 711, 796
Espaillat C. et al. 2007, ApJ, 670, L135
Fabian A.C., Rees M.J., Stella L. & White N.E., 1989, MNRAS, 238, 729
Farris B.D., Duffell P., MacFadyen A.I. & Haiman Z., 2013, MNRAS, arXiv:1310.0492
Ford K. E.S., McKernan B., Sivaramakrishnan A., Martel

A., Koekemoer A. & Lafreniere D., 2013, ApJ, accepted, arXiv:1401.0545
Gierliński M. & Done C., 2004, MNRAS, 349, L7
Gould A. & Quillen A.C., 2003, ApJ, 592, 935
Gültekin K. & Miller J.M., 2012, ApJ, 761, 90
Haiman Z., Kocsis B., Menou K., Lippai Z. & Frei Z. 2008, ASPC, 399, 20
Hansen B.M.S. & Milosavljević M., 2003, ApJ, 593, L77
Hayasaki K., Mineshige S. & Ho L.C., 2008, ApJ, 582, 1134
Hills J.G., 1988, Nature, 331, 687
Ho L.C. 2008, ARA&A, 46, 475
Hobbs A. & Nayakshin S., 2009, MNRAS, 394, 191
Huerta E.A. & Gair J.R. 2011, PRD 83, 044021
Ivanov P.B., Papaloizou J.C.B. & Polnarev A.G., 1999, MNRAS, 307, 79
Jang-Condell H. & Sasselov D.D., 2003, ApJ, 593, 1116
Ju, W., Greene J.E., Rafikov R.R., Bickerton S.J. & Badenes C., 2013, ApJ submitted, arxiv:1306.4987
Kocsis B. & Levin J. 2012, PRD, 85, 123005
Kocsis B., Frei Z., Haiman Z., & Menou K. 2006a, ApJ, 637, 27
Kocsis B., Gáspár M.E., Márka S. 2006b, ApJ, 648, 411
Kocsis B., Haiman Z., Menou K., & Frei Z. 2007, PRD, 76, 022003
Kocsis B., Haiman Z., & Menou K. 2008, ApJ, 684, 870
Kocsis B., Yunes N., & Loeb A. 2011, PRD, 84, 024032
Kocsis B., Haiman Z. & Loeb A., 2012a, MNRAS, 427, 2660.
Kocsis B., Haiman Z. & Loeb A., 2012b, MNRAS, 427, 2680.
Kormendy J. & Richstone D., 1995, ARA&A, 33, 581
Lang R.N. & Hughes S.A. 2008, ApJ, 677, 1184
Lang R.N., Hughes S. A., & Cornish N.J. 2011, PRD, 84, 022002
Levin Y. 2006, ApJ, 653, 1203
Lewis K.T., Eracleous M. & Storchi-Bergmann T., 2010, ApJS, 187, 416
Lin D.N.C. & Papaloizou J., 1986, ApJ, 309, 846
Liu F.K., Wu X.-B. & Cao S.L., 2003, MNRAS, 340, 411
Madigan A.-M., Levin Y. & Hopman C., 2009, ApJ, 697, L44
Madigan A.-M., Hopman C. & Levin Y., 2011, ApJ, 738, 99
Maiolino R. et al., 2010, A&A, 517, 47
Masset F.S. & Papaloizou J.C.B., 2003, ApJ, 588, 494
Maoz D., Nagar N.M., Falcke H. & Wilson A.S., 2005, ApJ, 625, 699
Mikóczi B., Kocsis B., Forgács P., & Vasúth, M., 2012, PRD, 86, 4027
Milosavljevic M. & Phinney E.S., 2005, ApJ, 622, L93
McKernan B. & Yaqoob T., 1998, ApJ, 501, L29
McKernan B. & Yaqoob T., 2004, ApJ, 608, 157
McKernan B., Yaqoob T. & Reynolds C. S., 2007, MNRAS, 379, 1359
McKernan B., Maller A.H.& Ford, K.E.S., 2010a, ApJ, 718, L83
McKernan B., Ford, K.E.S. & Reynolds C.S., 2010b, MNRAS, 407, 2399
McKernan B., Ford, K.E.S., Lyra W., Perets H.B., Winter L.M. & Yaqoob T., 2011a, MNRAS, 417, L103
McKernan B., Ford, K.E.S., Yaqoob T. & Winter L.M., 2011b, MNRAS 413, L24
McKernan B., Ford, K.E.S., Lyra W. & Perets H.B., 2012, MNRAS, 425, 460 (Paper I)
McKernan B., Ford, K.E.S., Kocsis B. & Haiman Z., 2013, MNRAS, 432, 1468
Miller M.C. & Hamilton D.P., 2002, MNRAS, 330, 232
Naoz S., Kocsis B., Loeb A., & Yunes N. 2013, ApJ, 773, 187
Nardini E., Fabian A.C. & Walton D.J., 2012, MNRAS (accepted), astro-ph/1204.4451
Nayakshin S. & Sunyaev R., 2007, MNRAS, 377, 1647
Nissanke S., Holz D.E., Hughes S.A., Dalal N., &Sievers J.L., 2010, ApJ, 725, 496
Nissanke S., Sievers J., Dalal N., & Holz D., 2011, ApJ, 739, 99
Nixon C.J., Cossins P.J., King A.R. & Pringle J.E., 2011, MNRAS, 412, 1591
O'Leary R. M., Kocsis B. & Loeb A. 2009, MNRAS, 395, 2127
Pepliński A., Artymowicz P. & Mellema G., 2008a, MNRAS, 386, 164
Pepliński A., Artymowicz P. & Mellema G., 2008b, MNRAS, 387, 1063
Peters P.C. & Mathews J. 1963, Phys. Rev., 131, 435
Peters P.C., 1964, Phys. Rev., 136, 1224
Peterson B.M., 1993, PASP, 105, 247
Pollack J.B., Hubickyj O., Bodenheimer P., Lissauer J.J., Podolak M. & Greenzweig Y., 1996, Icarus, 124, 62
Preibisch T. et al., 2005, ApJS, 160, 401
Rafikov R.R., 2012, arXiv:1205.5017
Remillard R.A. & McClintock J.E., 2006, ARA&A, 44, 49
Reynolds C.S., 1997, MNRAS, 286, 513
Rivers E., Markowitz A. & Rothschild R., 2011, ApJ, 742, L29
Roedig C., Sesana A., Dotti M., Cuadra J., Amaro-Seoane P. & Haardt F., 2012, MNRAS (submitted), arXiv:1202.6063
Samsing J., MacLeod M., Ramirez-Ruiz E., 2013, ApJ submitted, arXiv:1308.2964
Scott A.E., Stewart G.C. & Mateos S. 2012, MNRAS, 423, 2633
Shakura N.I. & Sunyaev R.A. 1973, A&A, 24, 337
Sirko E. & Goodman J. 2003, MNRAS, 341, 501
Strader J., Chomiuk L., Maccarone T.J., Miller-Jones J.C.A., Seth A.C., Heinke C.O. & Sivakoff G.R., 2012, ApJ, 750, L27
Strateva I.V. et al. 2003, AJ, 126, 1720
Subr L. & Karas V. 2005, A&A, 433, 405
Syer D. & Clarke C.J. 1995, MNRAS, 277, 758
Turner T.J., Reeves J.N., Kraemer S.B. & Miller L. 2008, A&A, 483, 161
van den Heuvel E.P.J., Bhattacharya D., Nomoto K. & Rappaport S.A. 1992, A&A, 262, 97
Veitch J., Mandel I., Aylott B., Farr B., Raymond V., Rodriguez C., van der Sluys M., Kalogera V., & Vecchio A. 2012, PRD, 85, 104045
Veron-Cetty M.-P. & Veron P. 2006, A&A, 455, 773
Winter L.M., Mushotzky R.F., Reynolds C.S. & Tueller J. 2009, ApJ, 690, 1322
Winter L.M., Veilleux S., McKernan B. & Kallman T. 2012, ApJ, 745, 107
Yu Q. & Tremaine S. 2003, ApJ, 599, 1129
Yu Q., Lu H. & Lin D.N.C. 2007, ApJ, 666, 919
Yunes N., Kocsis B., Loeb A., & Haiman Z. 2011, PRL, 107, 171103
Yunes N., Miller M.C., Thornburg J. 2011, PRD, 83, 044030
Zentsova A.S., 1983, Astrophys. Space Sci., 95, 11
Zheng W. et al. 1995, ApJ, 444, 632
Zhu Z., Stone J. M. & Rafikov R.R., 2013, ApJ, 768, 143